Efficient and Accurate Full-Wave Analysis of the Open-Ended Coaxial Cable

Gaetano Panariello, Luigi Verolino, and Gaetano Vitolo

***Abstract*—An efficient implementation of the full-wave open-ended-coaxial-line analysis is presented in this paper. The involved integrals are approached in such a way that the admittance is accurately calculated. Moreover, the calculus time is noticeably reduced. This technique is particularly useful when repeated analysis are performed as occurs, e.g., when measuring permittivity.**

***Index Terms*—Coaxial cable, permittivity measurements, termination.**

I. Introduction

THE open-ended coaxial probe is a useful tool to perform permittivity measurements [1]–[6] since it offers many advantages with respect to classical methods: the measure is noninvasive and requires a small sensing area in a broad band. Permittivity measurement requires the analysis of the reflection coefficient of the fundamental mode when the probe is in contact with the material under test.

Many authors approached the problem by using approximate formulations; some of them [1], [7] use an equivalent lumped-element circuit, others [8] use a virtual line model. The field analysis is approached in different ways: the main problem is to describe the electromagnetic field on the termination plane: some authors [9], [10] use only the fundamental mode, others [11], [12] take into account higher order modes. The drawback of the first strategy is that approximate models are valid only in restricted frequency and probe-dimension range. The second way to approach the problem is more general, but, up to now, has been too time consuming in order to perform online measurements.

A third strategy has been proposed by Stuchly *et al.* [13], and Anderson *et al.* [14]. They assume that the probe admittance is a rational function of the square root of the product permittivity frequency, whose coefficients are determined by calculating the admittance itself for various dielectrics. The drawback of this technique is that it has some limitations regarding the permittivity range and, in principle, it does not work in the presence of conductivity. Moreover, the coefficients provided are valid for restricted geometries.

Manuscript received August 3, 1999; revised December 22, 2000.

G. Panariello was with the Department of Electronic and Telecommunication Engineering, University of Naples Federico II, I-80125 Naples, Italy. He is now with the Department of Automation, Electromagnetism, Information Engineering, and Industrial Mathematics, University of Cassino, 03043 Cassino, Italy.

L. Verolino is with the Department of Electrical Engineering, University of Naples Federico II, I-80125 Naples, Italy (e-mail: verolino@unina.it).

G. Vitolo was with the Department of Electronic and Telecommunication Engineering, University of Naples Federico II, I-80125 Naples, Italy. He is now with Lucent Technologies, 00148 Rome, Italy.

Publisher Item Identifier S 0018-9480(01)05039-6.

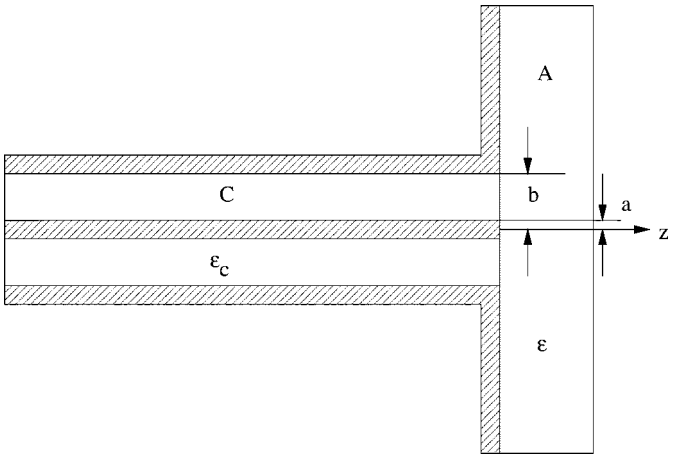

Fig. 1. Probe description.

The aim of this paper is to illustrate a fast and accurate technique to analyze the open-ended coaxial probe. A full-wave analysis is performed based on a modal representation of the field inside the cable and on a spectral one in the dielectric medium. This formulation has been used by many authors, [12], [15], but it could not be used to perform online permittivity measurements because the evaluation of the integrals involved is too time consuming. In this paper, a technique is shown to calculate them accurately and efficiently so that the admittance calculus is noticeably reduced.

II. Admittance Calculus

Consider the probe depicted in Fig. 1. The coaxial cable (C region) is filled by a dielectric of permittivity ϵ_c. The cable is truncated at $z = 0$, is indefinite toward the direction of the negative z, and is in contact with a dielectric medium characterized by permittivity ϵ. Let us suppose that the fundamental-mode is impinging from $z = -\infty$.

In order to obtain an equation for the probe admittance, we can represent the tangential field components in the C and A regions with a suitable base and match them on the interface. Due to the azimuthal symmetry of the structure and of the excitation, the field does not depend upon the ϕ coordinate and it is TM.

The field in the C region can be represented by the modal expansion and only TM^{0n} modes must be considered [11] as follows:

$$E_\rho = \psi_0(\rho)e^{-jk_0 z} + \sum_{n=0}^{\infty} c_n \psi_n(\rho) e^{jk_n z} \tag{1}$$

$$H_\phi = Y_0 \psi_0(\rho)e^{-jk_0 z} - \sum_{n=0}^{\infty} Y_n c_n \psi_n(\rho) e^{jk_n z} \tag{2}$$

where the modal functions are defined by the following equations:

$$\psi_0(\rho) = N_0 \frac{1}{\rho} \tag{3}$$

$$\psi_n(\rho) = N_n \left[J_1\left(\gamma_n \frac{\rho}{a}\right) Y_0(\gamma_n) - Y_1\left(\gamma_n \frac{\rho}{a}\right) J_0(\gamma_n) \right] \tag{4}$$

γ_n are the eigenvalues, which are solutions of the following:

$$J_0\left(\gamma_n \frac{b}{a}\right) Y_0(\gamma_n) = Y_0\left(\gamma_n \frac{b}{a}\right) J_0(\gamma_n) \tag{5}$$

and the normalizing constants providing the orthogonal property

$$\int_a^b \rho \psi_n(\rho) \psi_m(\rho)\, d\rho = \delta_{n,\,m} \tag{6}$$

are the following:

$$N_0 = \left[\ln(b/a)\right]^{-(1/2)} \tag{7}$$

$$N_n = \frac{\pi \gamma_n}{\sqrt{2}a} \left[\frac{J_0^2(\gamma_n)}{J_0^2(\gamma_n b/a)} - 1 \right]^{-(1/2)}. \tag{8}$$

The field in the A region can be represented in the spectral domain. The Hankel-transformed longitudinal electric field [16] satisfying the Helmholtz equation under an infinity radiation condition is

$$\mathcal{E}_z(w,\, z) = A(w) e^{-j\beta(w) z} \tag{9}$$

where $\beta(w) = \sqrt{k^2 - w^2}$, $A(w)$ is an unknown function and the square-root branch is the one that provides the negative imaginary part ($\pi \le \angle\beta \le 2\pi$). The field transverse components can be expressed by means of the longitudinal ones, and the result is as follows:

$$E_\rho = j \int_0^\infty \beta(w) A(w) e^{-j\beta(w) z} J_1(w\rho)\, dw \tag{10}$$

$$H_\phi = j\omega\epsilon \int_0^\infty A(w) e^{-j\beta(w) z} J_1(w\rho)\, dw. \tag{11}$$

Tangential-field components are continuous across the interface, i.e., for $z = 0$. Moreover, the tangential electric-field component vanishes on the flange and on the inner conductor of the coaxial cable, i.e., for $b < \rho$ and $\rho < a$. The following equations are obtained by matching the representations of the field components (1), (2), (10), and (11):

$$j\omega\epsilon \int_0^\infty A(w) J_1(w\rho)\, dw = Y_0 \psi_0(\rho) - \sum_{n=0}^{\infty} Y_n c_n \psi_n(\rho), \qquad \text{if } a \le \rho \le b \tag{12}$$

$$j \int_0^\infty \beta(w) A(w) J_1(w\rho)\, dw = \begin{cases} 0, & \text{if } \rho < a \\ \psi_0(\rho) + \sum_{n=0}^{\infty} c_n \psi_n(\rho), & \text{if } a \le \rho \le b \\ 0, & \text{if } b < \rho. \end{cases} \tag{13}$$

Equations (12) and (13) must be simultaneously solved to obtain the reflection coefficient c_0. Equation (13) can be interpreted as an inverse Hankel transform [16] and, therefore,

$$A(w) = -j \frac{w}{\beta(w)} \left[\Psi_0(w) + \sum_{n=0}^{\infty} c_n \Psi_n(w) \right] \tag{14}$$

where

$$\Psi_n(w) = \int_a^b \rho \psi_n(\rho) J_1(w\rho)\, d\rho. \tag{15}$$

Algebraic manipulations enables us to write that

$$\Psi_n(w) = A_n a f_n(wa) \tag{16}$$

where

$$f_n(x) = \frac{x}{x^2 - \gamma_n^2} \left[J_0(\gamma_n r) J_0(x) - J_0(\gamma_n) J_0(rx) \right] \tag{17}$$

$r = b/a$, $\gamma_0 = 0$, and the constants A_n are related to N_n. Thus, we can multiply (12) by $\rho\psi_m(\rho)$ and integrate over the aperture; considering orthonormal properties of the modal functions (6) and substituting the expression for $A(w)$ given by (14), we obtain

$$c_m \frac{\epsilon_c}{\epsilon k_m a} + \sum_{n=0}^{\infty} c_n A_n A_m I_{nm} = \frac{\epsilon_c}{\epsilon k_0 a} \delta_{0,\,m} - A_0 A_m I_{0m}, \qquad \text{for } m = 0,\, 1,\, \ldots \tag{18}$$

where

$$I_{nm} = \int_0^\infty \frac{x}{\sqrt{\kappa^2 - x^2}} f_n(x) f_m(x)\, dx \tag{19}$$

and for shortness, we called $\kappa = ka$. Let

$$M_{nm} = \frac{\epsilon_c\, \delta_{n,\,m}}{\epsilon k_n a} + A_n A_m I_{nm} \tag{20}$$

$$b_n = A_n A_0 I_{n0}. \tag{21}$$

From (18), we finally obtain the following equation that provides the normalized aperture admittance:

$$Y = \frac{1 - c_0}{1 + c_0} = \frac{\epsilon k_0 a}{\epsilon_c} \left(A_0^2 I_{00} - \mathbf{b^T M^{-1} b} \right). \tag{22}$$

From a numerical point-of-view, the most delicate point is the evaluation of integrals (19), and we could not find an exhaustive discussion in the literature on their calculus; the aim of Section III is to address this problem.

III. Integral Calculus

The integrals of (19) are defined over an infinite range; the integrand functions decay, for large x, as x^{-3}, exhibiting an oscillatory behavior due to the Bessel function J_0. Moreover, they have a singularity-like behavior (a true singularity if the medium under test is lossless) when x^2 approaches $\Re\{\kappa^2\}$. For the aforementioned, it is convenient to transform them to obtain a less cumbersome computation.

First of all, we extract the asymptotic behavior from the integrand functions; more precisely, noting that, for large x, the following approximation holds:

$$\frac{x}{\sqrt{\kappa^2 - x^2}} \sim j \left(1 + \frac{\kappa^2}{2x^2} \right) \tag{23}$$

we obtain

$$I_{nm} = jI^{\infty}(\gamma_n, \gamma_m) + \delta I_{nm} \tag{24}$$

where we introduced the notations

$$I^{\infty}(\gamma_n, \gamma_m) = \int_0^{\infty} \left(1 + \frac{\kappa^2}{2x^2}\right) f_n(x) f_m(x)\, dx \tag{25}$$

$$\delta I_{nm} = \int_0^{\infty} \left[\frac{x}{\sqrt{\kappa^2 - x^2}} - j\left(1 + \frac{\kappa^2}{2x^2}\right)\right] \cdot f_n(x) f_m(x)\, dx. \tag{26}$$

Note that the integrand function of (26) decays as fast as x^{-7}.

As a second task, we extract the singularity-like behavior of the integrand function of (26), adding and subtracting from the integrand the following function:

$$A\frac{x}{\sqrt{\kappa^2 - x^2}}\, e^{-j\sqrt{\kappa^2 - x^2}} \tag{27}$$

where A is a suitable constant chosen to exactly subtract the singularity-like behavior. The function (27) can be analytically integrated and the result is $jAe^{-j\kappa}$.

Note that the more $|\kappa|$ decreases, the more integrals (26) are small compared with (25) since approximation (23) is always more exact. Therefore, it is very important to accurately calculate (25). However, the integral (25) suffers from the same problems of (19) and, therefore, a numerical evaluation is rather difficult. In the following, we show a technique to solve this problem. We point out that (19) can be expressed by a sum of integrals not depending on permittivity and, thus, by integrals that can be evaluated once for a fixed geometry.

If we examine the expression f_n, we can note that, for $n, m > 0$, but $n \neq m$, (25) can be expressed by summing integrals of simpler functions as follows:

$$\mathcal{I}(\gamma_n, \boldsymbol{\alpha}_i) = \int_0^{\infty} \frac{1}{x^2 - \gamma_n^2}\, J_0(\alpha_{i1}x) J_0(\alpha_{i2})\, dx \tag{28}$$

where $\boldsymbol{\alpha}_0 = (1, 1)$, $\boldsymbol{\alpha}_1 = (1, r)$, and $\boldsymbol{\alpha}_2 = (r, r)$. Moreover, using the equality 6.684.1 [17] and [18, eq. (32)], (28) becomes

$$\mathcal{I}(\gamma_n, \boldsymbol{\alpha}_i) = -\frac{1}{2\gamma_n} \int_0^{\pi} \mathcal{H}_0\left[\gamma_n\, d(\boldsymbol{\alpha}_i, \theta)\right] d\theta \tag{29}$$

where $\mathcal{H}_0$ is the zeroth-order Struve function, and

$$d(\boldsymbol{\alpha}_i, \theta) = \sqrt{\alpha_{i1}^2 + \alpha_{i2}^2 - 2\alpha_{i1}\alpha_{i2}\cos\theta}. \tag{30}$$

In order to calculate $I^{\infty}(\gamma_n, \gamma_n)$, $I^{\infty}(\gamma_n, 0)$, and $I^{\infty}(0, 0)$, we perform the following limits:

$$I^{\infty}(\gamma_n, \gamma_n) = \lim_{\gamma_m \to \gamma_n} I^{\infty}(\gamma_n, \gamma_m) \tag{31}$$

$$I^{\infty}(\gamma_n, 0) = \lim_{\gamma_m \to 0} I^{\infty}(\gamma_n, \gamma_m) \tag{32}$$

$$I^{\infty}(0, 0) = \lim_{\substack{\gamma_n \to 0 \\ \gamma_m \to 0}} I^{\infty}(\gamma_n, \gamma_m). \tag{33}$$

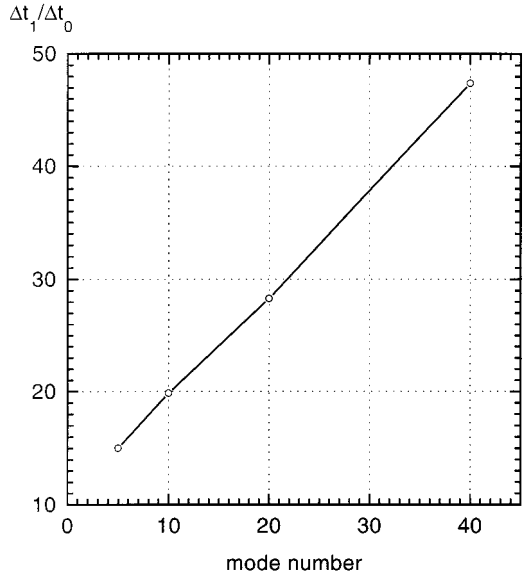

Fig. 2. Gain in evaluating matrix M, Δt_1, and Δt_0 are, respectively, the elapsed times to calculate integrals (19) and (24).

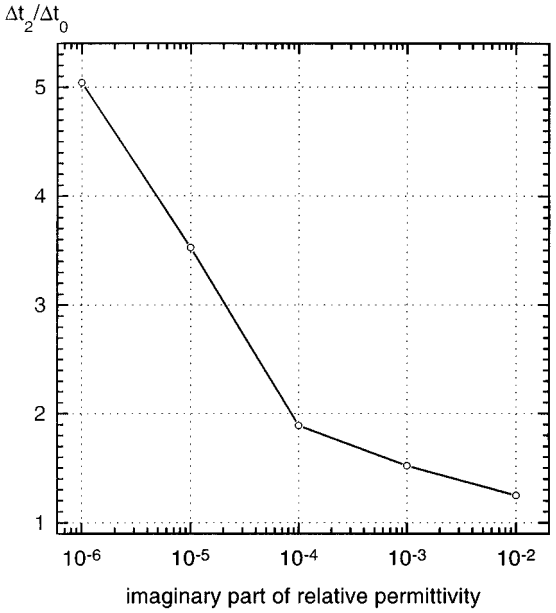

Fig. 3. Singularity behavior where Δt_2 and Δt_0 are, respectively, the elapsed times to calculate (19) without and with the singularity extraction.

The results are summarized in the Appendix. It can be noted that the integrals (25) are calculated by summing integrals of well-behaved functions over a compact range. Moreover, every integral depends only on the geometry and, thus, the calculus is needed only once for any given probe.

To estimate the gain obtained with this technique, we evaluated the matrix $\mathbf{M}$ for $f = 10$ GHz, $\epsilon = (3 - j0.1)\epsilon_0$, $\epsilon_c = 2.1\epsilon_0$ (Teflon), $b/a = 3.268$, $Z_0 = 50\ \Omega$ considering a number of modes from 1 up to 40. The improvement obtained with the technique presented here is significant, as shown in Fig. 2. The calculus is 20 time faster even with ten modes. Fig. 3 demonstrates that the singularity-like behavior gives less cumbersome computation and problems arise only when the losses are very

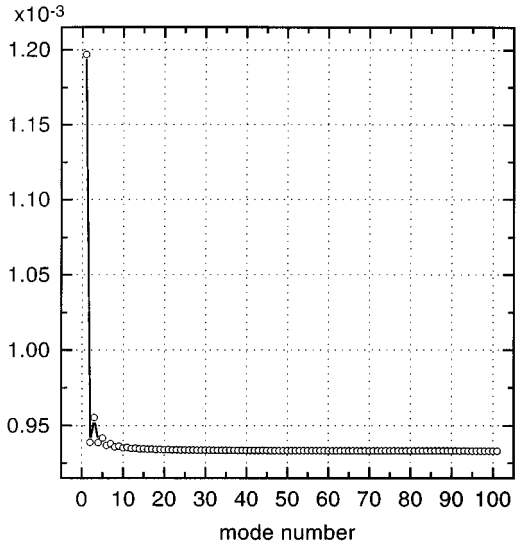

Fig. 4. Real part of normalized admittance versus the mode number.

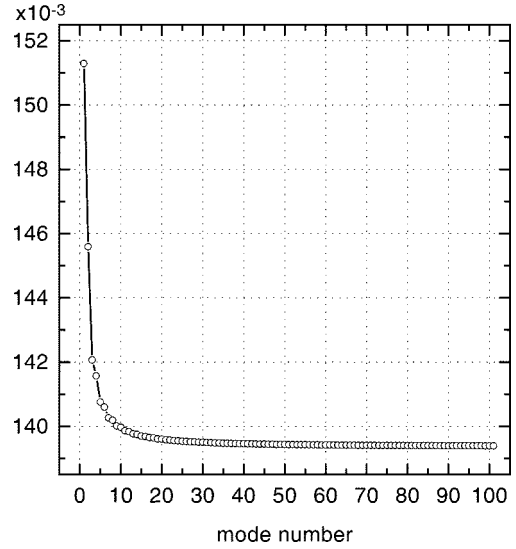

Fig. 5. Imaginary part of normalized admittance versus the mode number.

small. The behavior for large x is the main reason for the difficulties in evaluating (19).

IV. Results and Discussion

To examine the validity of the formulation, some numerical simulations have been performed. First of all, we investigated the convergence of the admittance calculus. We tried to evaluate the number of modes needed to accurately calculate the admittance: this is not an easy task. In order to answer this question, we calculated the admittance with the following data: $\epsilon = 2.1$ (Teflon), $f = 10$ GHz, $b/a = 3.268$, and $Z_0 = 50\ \Omega$, varying the mode number considered to represent the field. The results are depicted in Figs. 4 and 5. These figures show that we can assume the admittance calculated with 100 modes to be the reference one.

Fig. 6 shows the relative errors obtained with a smaller number of modes and with the rational function expression [14]. Note that the rational function gives an error just a bit bigger than that obtained with six modes, despite the expression being quite simple.

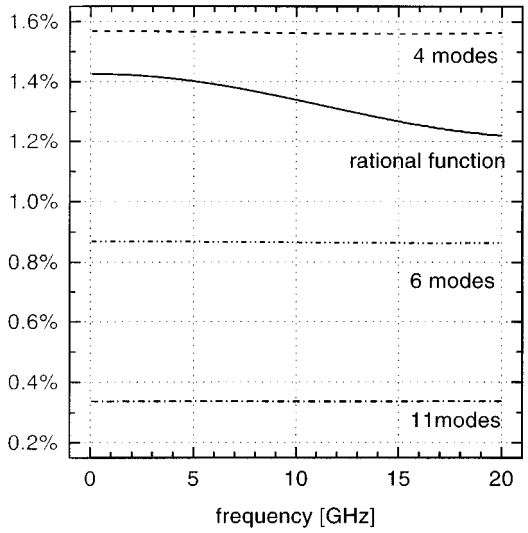

Fig. 6. Normalized admittance relative error (Teflon).

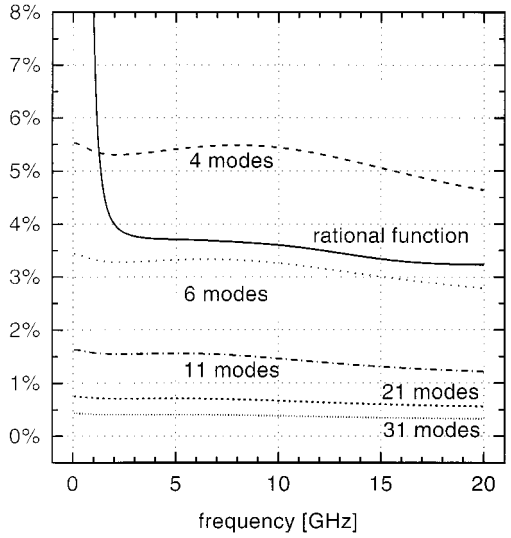

Fig. 7. Normalized admittance relative error (saline solution).

The error depends on the permittivity of the medium. To evaluate this, we analyze a very different one: saline solution $0.5N$ [19]. It exhibits a very high permittivity and, since it is a ionic solution, a conductivity. The relative error is depicted by Fig. 7: it is higher than the Teflon case. Moreover, we can note that, as expected, the rational function formulation error is very high at low frequencies, where the conductivity of the medium is significant. Therefore, it cannot be used to analyze ionic solutions like biological media.

V. Conclusions and Perspectives

This paper has addressed the accurate and efficient evaluation of the admittance of the flanged coaxial cable. In Section III (details in the Appendix), the calculus of the involved integrals is deeply discussed and a technique is presented to evaluate them. The reduction of the calculus time is considerably high, even with a low number of modes. The accuracy is very high since the permittivity-dependent terms are small compared with the geometry-dependent ones, evaluated integrating well-behaved

functions over a compact range. Moreover, if a probe facing a stratified medium is concerned, the formulation leads to integration of functions having exactly the same asymptotic behavior. Therefore, the integral evaluation discussed in Section III is still valid in the more general case.

In Section IV, some result are presented, showing that ten modes are sufficient to describe the admittance of the probe with a small error.

We hope, in the near future, to employ these results to develop a fast and accurate inversion algorithm in order to obtain permittivity from measured admittance data values.

APPENDIX
INTEGRAL CALCULUS RESULTS

The following equations summarize the results of the manipulations described in Section III:

$$I^{\infty}(\gamma_n, \gamma_m) = \sum_{i=0}^{2} \lambda_{nm}^{(i)} \mathcal{I}(\gamma_n, \boldsymbol{\alpha}_i) + \lambda_{mn}^{(i)} \mathcal{I}(\gamma_m, \boldsymbol{\alpha}_i) \quad (34)$$

where

$$\lambda_{nm}^{(0)} = J_0(r\gamma_n) J_0(r\gamma_m) \frac{\gamma_n^2 + \frac{1}{2}\kappa^2}{\gamma_n^2 - \gamma_m^2} \quad (35)$$

$$\lambda_{nm}^{(1)} = -\Big[J_0(r\gamma_n) J_0(\gamma_m) + J_0(r\gamma_m) J_0(\gamma_n) \Big] \cdot \frac{\gamma_n^2 + \frac{1}{2}\kappa^2}{\gamma_n^2 - \gamma_m^2} \quad (36)$$

$$\lambda_{nm}^{(2)} = J_0(\gamma_n) J_0(\gamma_m) \frac{\gamma_n^2 + \frac{1}{2}\kappa^2}{\gamma_n^2 - \gamma_m^2} \quad (37)$$

$$I^{\infty}(\gamma_n, \gamma_n) = \sum_{i=0}^{2} 2(-1)^i \binom{2}{i} J_0^i(\gamma_n) J_0^{2-i}(r\gamma_n) \left[1 - \frac{\kappa^2}{2\gamma_n^2} \right] \cdot \left[\left(1 - \frac{\kappa^2}{2\gamma_n^2} \right) \mathcal{I}_n(\boldsymbol{\alpha}_i) + \left(1 + \frac{\kappa^2}{2\gamma_n^2} \right) \mathcal{J}_n(\boldsymbol{\alpha}_i) \right] \quad (38)$$

$$I^{\infty}(\gamma_n, 0) = \sum_{i=0}^{2} \left[J_0(r\gamma_n) \frac{3i^2 - 7i + 2}{2} + J_0(\gamma_n) \frac{3i^2 - 5i}{2} \right] \cdot \left[\left(1 + \frac{\kappa^2}{2\gamma_n^2} \right) \mathcal{I}_n(\boldsymbol{\alpha}_i) + \frac{\kappa^2}{2\gamma_n^2} \mathcal{E}(\boldsymbol{\alpha}_i) \right] \quad (39)$$

$$I^{\infty}(0, 0) = \sum_{i=0}^{2} \left(3i^2 - 6i + 1 \right) \left[\frac{1}{18} \kappa^2 \mathcal{F}(\boldsymbol{\alpha}_i) - \mathcal{E}(\boldsymbol{\alpha}_i) \right] \quad (40)$$

$$\mathcal{J}(\gamma_n, \boldsymbol{\alpha}_i) = \frac{1}{2} \int_0^{\pi} d(\boldsymbol{\alpha}_i, \theta) \left[\mathcal{H}_1\Big(\gamma_n\, d(\boldsymbol{\alpha}_i, \theta) \Big) - 1 \right] d\theta \quad (41)$$

$$\mathcal{E}(\boldsymbol{\alpha}_i) = \frac{1}{\pi} \int_0^{\pi} d(\boldsymbol{\alpha}_i, \theta)\, d\theta \quad (42)$$

$$\mathcal{F}(\boldsymbol{\alpha}_i) = \frac{1}{\pi} \int_0^{\pi} d^3(\boldsymbol{\alpha}_i, \theta)\, d\theta. \quad (43)$$

$\mathcal{H}_0$ and $\mathcal{H}_1$ are, respectively, the Struve function of zeroth and first orders and

$$\mathcal{E}(\boldsymbol{\alpha}_2) = \frac{4r}{\pi} \quad (44)$$

$$\mathcal{E}(\boldsymbol{\alpha}_1) = \frac{2(r-1)}{\pi} E\left[-\frac{4r}{(r-1)^2} \right] \quad (45)$$

$$\mathcal{F}(\boldsymbol{\alpha}_2) = \frac{32r^3}{3\pi} \quad (46)$$

$$\mathcal{F}(\boldsymbol{\alpha}_1) = \frac{2(r-1)}{3\pi} 4\left(1 + r^2\right) E\left[-\frac{4r}{(r-1)^2} \right] - \frac{2(r-1)}{3\pi} (1+r)^2 K\left[-\frac{4r}{(r-1)^2} \right] \quad (47)$$

where K and E are the complete elliptic integrals of the first and second kinds [20].

REFERENCES

[1] M. A. Stuchly and S. S. Stuchly, "Coaxial line reflection methods for measuring dielectric properties of biological substances at radio and microwave frequencies—A review," *IEEE Trans. Instrum. Meas.*, vol. IM-29, pp. 176–183, Sept. 1980.

[2] J. R. Mosig, J. E. Besson, M. Gex-Fabry, and F. E. Gardiol, "Reflection of an open-ended coaxial line and application to nondestructive measurement of materials," *IEEE Trans. Instrum. Meas.*, vol. IM-30, pp. 46–51, Mar. 1981.

[3] M. A. Stuchly, T. Whit Athey, G. M. Samaras, and G. E. Taylor, "Measurement of radio frequency permittivity of biological tissues with an open-ended coaxial line: Part II—Experimental results," *IEEE Trans. Microwave Theory Tech.*, vol. MTT-30, pp. 87–91, Jan. 1982.

[4] G. P. Oyyo and W. C. Chew, "Improved calibration of a large open-ended coaxial probe for dielectric measurements," *IEEE Trans. Instrum. Meas.*, vol. 40, pp. 742–746, Aug. 1991.

[5] Y. Xu, R. G. Bosisio, and T. K. Bose, "Some calculation methods and universal diagrams for measurement of dielectric constants using open-ended coaxial probes," *Proc. Inst. Elect. Eng.*, pt. H, vol. 138, pp. 356–360, Aug. 1991.

[6] H. Zheng and C. E. Smith, "Permittivity measurements using a short open-ended coaxial line probe," *IEEE Microwave Guided Wave Lett.*, vol. 1, pp. 337–339, Nov. 1991.

[7] T. Whit Athey, M. A. Stuchly, and S. S. Stuchly, "Measurement of radio frequency permittivity of biological tissues with an open-ended coaxial line: Part I," *IEEE Trans. Microwave Theory Tech.*, vol. MTT-30, pp. 82–86, Jan. 1982.

[8] F. M. Ghannouchi and R. G. Bosisio, "Measurement of microwave permittivity using a six-port reflectometer with an open-ended coaxial line," *IEEE Trans. Instrum. Meas.*, vol. 38, pp. 505–508, Apr. 1989.

[9] N. Marcuvitz, *Waveguide Handbook*. New York: McGraw-Hill, 1951.

[10] H. R. Levine and C. H. Papas, "Theory of the circular diffraction antenna," *J. Appl. Phys.*, vol. 22, pp. 29–43, 1951.

[11] C. W. Harrison, Jr. and D. C. Chang, "Theory of the annular slot antenna based on duality," *IEEE Trans. Electromagn. Compat.*, vol. EMC-13, pp. 8–14, Feb. 1971.

[12] C.-L. Li and K.-M. Chen, "Determination of electromagnetic properties of materials using flanged open-ended coaxial probe—Full-wave analysis," *IEEE Trans. Instrum. Meas.*, vol. 44, pp. 19–27, Feb. 1995.

[13] S. S. Stuchly, C. L. Sibbald, and J. M. Anderson, "A new aperture admittance model for open-ended waveguides," *IEEE Trans. Microwave Theory Tech.*, vol. 42, pp. 192–198, Feb. 1994.

[14] J. M. Anderson, C. L. Sibbald, and S. S. Stuchly, "A new aperture admittance model for open-ended waveguides," *IEEE Trans. Microwave Theory Tech.*, vol. 42, pp. 199–204, Feb. 1994.

[15] P. De Langhe, K. Blomme, L. Martens, and D. De Zutter, "Measurement of low-permittivity materials based on a spectral-domain analysis for the open-ended coaxial probe," *IEEE Trans. Instrum. Meas.*, vol. 42, pp. 879–886, Oct. 1993.

[16] A. D. Poularikas, Ed., *The Transforms and Applications Handbook*. Boca Raton, FL: CRC Press, 1995.

[17] I. S. Gradshteyn and I. M. Ryzhik, *Tables of Integrals, Series, and Products*, 5th ed. New York: Academic, 1994.
[18] A. P. Prudnikov, Y. A. Brychkov, and O. I. Marichev, *Integrals and Series*. New York: Gordon and Breach, 1992, vol. 2.
[19] A. Nyshadham, C. L. Sibbald, and S. S. Stuchly, "Permittivity measurements using open-ended sensors and reference liquid calibration—An uncertainty analysis," *IEEE Trans. Microwave Theory Tech.*, vol. 40, pp. 305–314, Feb. 1992.
[20] M. Abramowitz and I. A. Stegun, *Handbook of Mathematical Functions*. New York: Dover, 1970.

Gaetano Panariello was born in Herculaneum, Italy, in 1956. He received the Electronic Engineering degree (*summa cum laude*) and the Ph.D. degree from the University of Naples Federico II, Naples, Italy, in 1980 and 1989, respectively.

He was a Staff Engineer in the Antenna Division, Elettronica SpA, until 1984. He then joined the Electromagnetic Research Group, University of Naples Federico II, where he taught microwave circuit design as an Associate Professor in the Department of Electronic and Telecommunication Engineering. He is currently a Full Professor of electromagnetic field at The University of Cassino, Cassino, Italy. His research interests include inverse problems, nonlinear electromagnetic, analytical and numerical methods, and microwave circuit design.

Luigi Verolino was born in Naples, Italy, in 1960. He received the Electronic Engineering degree from the University of Naples Federico II, Naples, Italy, in 1980.

Until 1990, he was a Researcher at CERN, Geneva, Switzerland. He then joined the National Laboratories, National Institute for Nuclear Physics (INFN), Frascati, Italy. In 1992, he became a Researcher at the University of Naples Federico II, where, since 1998, he has been an Associate Professor. His research interests include accelerator beam dynamics, electromagnetic compatibility, printed structures, and nonlinear electromagnetic.

Gaetano Vitolo was born in Campobasso, Italy, on June 6, 1971. He received the Master degree (with honors) in electronic engineering from the University of Naples Federico II, Naples, Italy.

In 1996, he joined the Department of Electrical Engineering, University of Naples, Naples, Italy. He is currently with Lucent Technologies, Rome, Italy. His research interests include nondestructive testing of materials, permittivity measurements, numerical methods, microwave-induced polymerization, and microstrip passive device design.

Mr. Vitolo was the recipient of a 1996 research grant.